Journal of Medicinal Chemistry

Drug Annotation

pubs.acs.org/jmc

Discovery of 5-Chloro-4-((1-(5-chloropyrimidin-2-yl)piperidin-4-yl)oxy)-1-(2-fluoro-4-(methylsulfonyl)phenyl)pyridin-2(1*H*)-one (BMS-903452), an Antidiabetic Clinical Candidate Targeting GPR119

Dean A. Wacker,* Ying Wang, Matthias Broekema, Karen Rossi, Steven O'Connor, Zhenqiu Hong, Ginger Wu, Sarah E. Malmstrom, Chen-Pin Hung, Linda LaMarre, Anjaneya Chimalakonda, Lisa Zhang, Li Xin, Hong Cai, Cuixia Chu, Stephanie Boehm, Jacob Zalaznick, Randolph Ponticiello, Larisa Sereda, Song-Ping Han, Rachel Zebo, Bradley Zinker, Chiuwa Emily Luk, Richard Wong, Gerry Everlof, Yi-Xin Li, Chunyu K. Wu, Michelle Lee, Steven Griffen, Keith J. Miller, John Krupinski, and Jeffrey A. Robl

Departments of Discovery Chemistry, Metabolic Diseases, Lead Evaluation, Computer-Assisted Drug Design, Discovery Toxicology, Exploratory Clinical and Translational Research, and Pharmaceutical Candidate Optimization, Bristol-Myers Squibb, P.O. Box 5400, Princeton, New Jersey 08543-5400, United States

Supporting Information

ABSTRACT: G-protein-coupled receptor 119 (GPR119) is expressed predominantly in pancreatic β-cells and in enteroendocrine cells in the gastrointestinal tract. GPR119 agonists have been shown to stimulate glucose-dependent insulin release by direct action in the pancreas and to promote secretion of the incretin GLP-1 by action in the gastrointestinal tract. This dual mechanism of action has generated significant interest in the discovery of small molecule GPR119 agonists as a potential new treatment for type 2 diabetes. Herein, we describe the discovery and optimization of a new class of pyridone containing GPR119 agonists. The potent and selective BMS-903452 (**42**) was efficacious in both acute and chronic in vivo rodent models of diabetes. Dosing of **42** in a single ascending dose study in normal healthy humans showed a dose dependent increase in exposure and a trend toward increased total GLP-1 plasma levels.

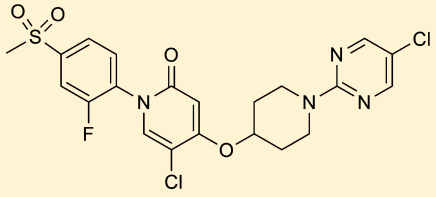

42

DISEASE TARGET

Diabetes is one of the fastest growing chronic diseases worldwide, with an estimated prevalence of 382 million patients, of which 85−95% have type 2 diabetes mellitus (T2DM).[1] T2DM is characterized by insufficient glycemic control due to insulin resistance and insufficient insulin secretion from the pancreas which leads to long-term complications such as heart disease, organ failure, and lower limb amputations.[2] Even though multiple pharmacological agents are available, less than one-third of T2DM patients achieve the desired glycemic control.[3] Furthermore, current treatments have efficacy limitations during long-term treatment and the potential for undesired side effects.[4] Therefore, new pharmacological treatments of T2DM with novel mechanisms of action are needed.

MECHANISM OF ACTION

The human body has multiple mechanisms that work in concert to properly control plasma glucose levels. Two of the most important of these mechanisms are insulin release from the pancreas and incretin hormone release (glucagon-like peptide 1 (GLP-1) and glucose-dependent insulinotropic polypeptide (GIP)) from the gastrointestinal tract. Elevation of plasma glucose induces insulin release from the pancreas, which in turn causes skeletal muscle and fat tissue to absorb glucose, thus lowering plasma levels. Meanwhile, nutrient intake and the concomitant elevation in blood glucose cause the incretin hormones to be released from the endocrine cells in the gastrointestinal tract. These hormones further enhance insulin secretion from the pancreas in a glucose dependent manner. GLP-1 has the added benefit of inhibiting glucagon release and decreasing gastric emptying to further reduce the glucose excursion. Additionally, rodent studies with GLP-1 have shown preservation of insulin releasing pancreatic islet β-cells.[5,6] Therefore, if a drug target could induce both insulin and incretin hormone release, more effective control of T2DM might be accomplished in a diabetic patient.

G-protein-coupled receptor 119 (GPR119) is a class A GPCR with little homology to other receptors and is expressed primarily in pancreatic β-cells and the K- and L-cells of the gastrointestinal tract.[7−10] In rodents, potent GPR119 agonists cause the release of insulin from pancreatic islets and increase insulin levels in vivo in a glucose dependent manner.[9] Also, in vivo studies in rodents have shown elevations in plasma levels of GLP-1 and GIP upon oral treatment with glucose with GPR119 agonists.[10] These results indicate GPR119 agonists have a dual mechanism for lowering plasma glucose levels and,

Received: July 31, 2014
Published: September 10, 2014

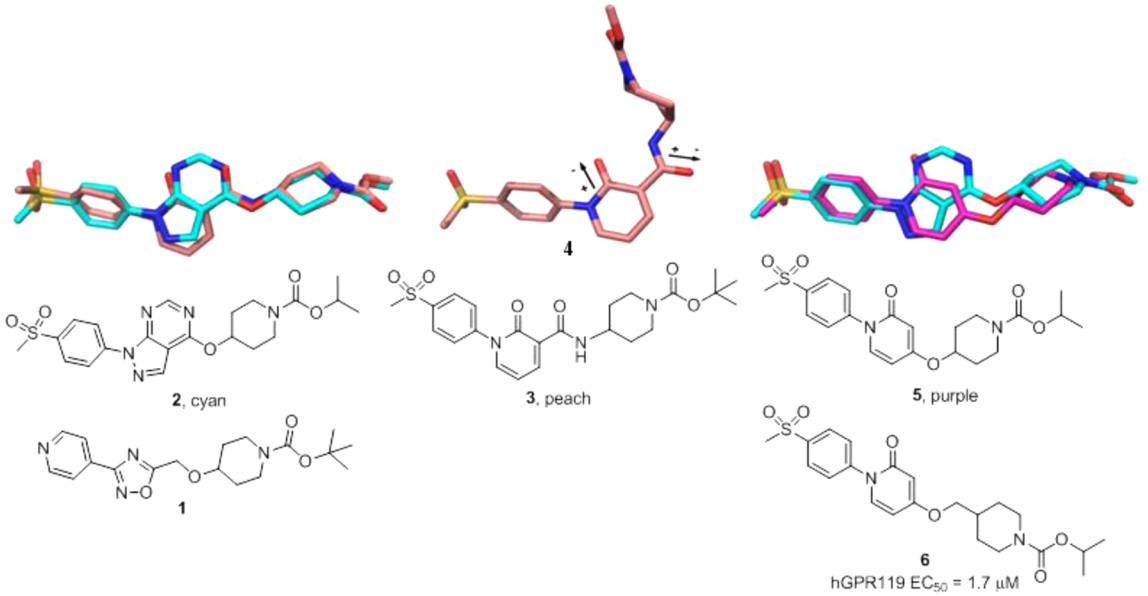

Figure 1. Pharmacophore overlays of GPR119 literature agonists and newly designed compounds.

therefore, have the potential to provide superior diabetes control over the current therapies.

COMPOUND DESIGN AND LEAD IDENTIFICATION

Our efforts to identify small molecule agonists of GPR119 were initiated with a high throughput screen (HTS) of our compound deck and pharmacophore modeling of GPR119 agonists disclosed by Prosidion Pharmaceuticals,[11] exemplified by **1**, and Arena Pharmaceuticals,[12] exemplified by **2**. These publications have inspired several companies to initiate discovery programs that have led to compounds entering clinic trials; Arena/Ortho-McNeil (APD668 and APD597),[13] Metabolex/Sanofi-Aventis (MBX-2982),[14,15] GlaxoSmithKline (GSK-1292263),[14,16] and Prosidion (PSN-821).[14,17] Although our HTS campaign identified some interesting structures, we were intrigued by the pharmacophore model built by overlaying low energy confirmations of both compounds (**1** and **2**). The pharmacophore model was used to determine the spatial orientation of left side aryl and right side piperidine functionality. We then designed multiple core structures that occupied the linker space and properly orientated the two terminal functionalities. The most interesting of the designed cores was the 1,3-substituted pyridone **3**. As can be seen in Figure 1, the aryl and piperidine overlay extremely well with the corresponding functionality in **2** (overlay of peach and cyan colored compounds) and the two carbonyls from **3** are located near the nitrogens of the pyrimidine core. However, when we went to the next step and analyzed the low energy conformations of **3**, we identified a flaw in our design. The low energy conformation of **3** minimizes the overall dipole moment of the compound and thus rotates the exocyclic amide 180° from desired conformation, as can been seen in structure **4**. We therefore needed to redesign the molecule to a 1,4-substitution of the pyridone ring, **5**, to identify a low energy confirmation that overlaid well with **2** (as can be seen in the purple compound overlay with the cyan compound). Synthesis of the methylene analog **6** provided our first active compound in this series.

Our initial efforts focused on improving the in vitro potency of the lead molecule **6**. Replacement of the methylene piperidine linker with a wide variety of nitrogen heterocycles provided few compounds with improved potency (Table 1). The incorporation of four- or five-membered rings (**7**–**10**) provided compounds that were inactive, and the azepine (**11**) was equivalent in potency to **6**. The first potency improvement came with the removal of the methylene between the oxygen and the piperidine ring which provided a compound (**5**) with

Table 1. In Vitro Activity of Linker Analogs

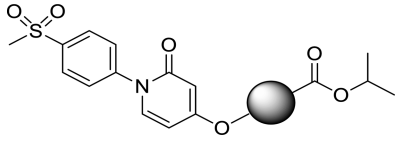

		hGPR119 EC_{50}, nM[a]	hGPR119 I.A.[b]
6	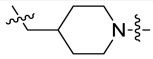	1700	0.7
7	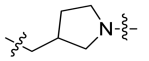	>10,000	
8	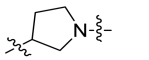	>10,000	
9	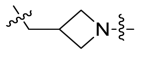	>10,000	
10	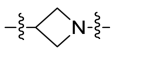	>10,000	
11	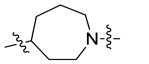	1091	0.7
5	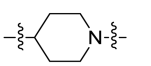	133	0.8
13	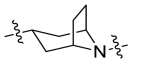	870	1.0
14	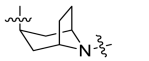	3500	0.7

[a] EC_{50} values were calculated from concentration–response curves. See ref 18 for assay conditions. [b] Reference compound set at 1.0 for each assay run.

dx.doi.org/10.1021/jm501175v | J. Med. Chem. 2014, 57, 7499–7508

~13-fold greater potency. We tried to further improve potency of the piperdine ring with conformational constraints by bridging the ring system (**13** and **14**); however, in each case the potency was reduced dramatically. Also, replacement of the oxygen in the linker with other heteroatoms or carbon was attempted and these modifications either dramatically reduced or eliminated all activity of the molecules (data not shown).

Further potency optimization at the terminal groups produced varying results. Replacement of the isopropyl carbamate with other carbamates provided compounds (**15**, **16**) of equivalent potency (Table 2). However, carbamate

Table 2. In Vitro Activity of Piperidine Analogs

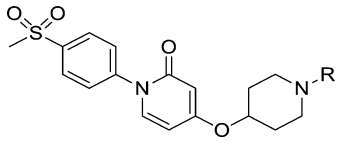

	R	hGPR119 EC_{50}, nM[a]	hGPR119 I.A.[b]
11	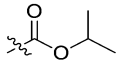	133	0.8
15	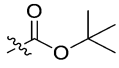	183	0.8
16	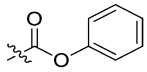	130	0.9
17	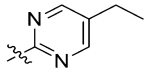	57	0.8
18	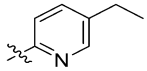	104	0.6
19	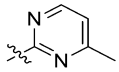	724	0.3
20	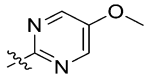	117	1.0
21	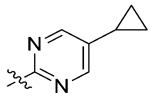	23	0.9
22	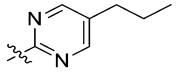	16	0.8

[a]EC_{50} values were calculated from concentration−response curves. See ref 18 for assay conditions. [b]Reference compound set at 1.0 for each assay run.

replacement with a pyrimidine (**17**) to mimic the oxygens increased potency by 2-fold. Incorporation of both heteroatoms was necessary to achieve the largest potency improvement, as shown by comparison to the pyridine (**18**). The substitution pattern of the pyrimidine ring was vital for retention of in vitro potency and efficacy, as can been seen with compounds **19** and **20**. The optimal potency substitutions were either cyclopropyl (**21**) or *n*-propyl (**22**) with increases of ~3-fold for each compound versus compound **17**. Even though an almost 10-fold increase in potency was achieved with piperidine modifications, potency increases from changes in the aryl substitution were more difficult to identify (Table 3). Substitution at the para position was vital; any movement of the group to the ortho or meta position ameliorated all activity

Table 3. In Vitro Activity of Phenyl Analogs

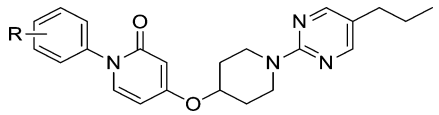

	R	hGPR119 EC_{50}, nM[a]	hGPR119 I.A.[b]
22	4-$MeSO_2$	16	0.8
23	4-MeSO	41	0.9
24	4-CN	11	0.8
25	4- 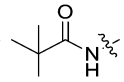	37	0.8
26	4- 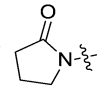	32	0.8
27	4- 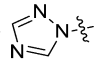	63	0.8
28	4- 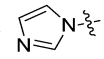	95	0.8
29	2-F-4-$MeSO_2$	18	1.0
30	3-F-4-$MeSO_2$	9	0.8

[a]EC_{50} values were calculated from concentration−response curves. See ref 18 for assay conditions. [b]Reference compound set at 1.0 for each assay run.

at GPR119 (data not shown). The only changes that provided compounds with reasonable potency either contained an amide group (**25**, **26**) or selected heterocyles (**27**, **28**). The only functional group that could replace the methyl sulfone and retain potency was cyano (**24**). Although 4-cyano compounds were potent, they typically exhibited lower aqueous solubility than the corresponding sulfone compounds. As will be discussed later in greater detail, solubility limited absorption was an issue for the program, and therefore, we deemphasized cyano compounds in the SAR program. Substitutions at the ortho and meta positions of the aryl were tested in conjunction with the methyl sulfone. Potency increases were not identified, but small functionality was tolerated, such as fluoro (**29**, **30**), chloro, and methyl. Incorporation of large groups, such as phenyl, resulted in a dramatic loss of all potency.

With in vitro potency goals met, we wanted to identify issues related to druglike properties for this series of compounds. Compound **29** was chosen for evaluation in our in vitro safety and metabolism assays in addition to pharmacokinetic evaluation in mice. The molecule exhibited an excellent profile in most of the safety assays: minimal inhibition (IC_{50} > 40 μM) at nine different cytochrome P450 enzymes, no activation of PXR (EC_{50} > 50 μM), and no cytotoxicity in a heptatic (HEPG2) cell line at a concentration of 40 μM. Compound **29** was tested against a panel of 43 different GPCRs and enzymes and showed minimal activity (<50% activity) at concentrations below 20 μM. The compound weakly inhibits the hERG channel in a patch clamp assay (47% at 10 μM). Compound **29** has excellent permeability in both the PAMPA (320 nm/s) and Caco2 assays (220 nm/s). In a human liver microsome stability assay, **29** has a half-life of 31 min. The compound is highly protein bound in rodent and human plasma (99% bound) and

dx.doi.org/10.1021/jm501175v | J. Med. Chem. 2014, 57, 7499−7508

has pH dependent solubility of 6 μg/mL at pH 6.5 and 630 μg/mL at pH 1.0. With good overall in vitro characteristics, **29** was dosed as an oral suspension to C57BL/6 mice at 30 mg/kg. The compound achieved a maximum plasma concentration of 38.6 μM at 2 h after dose with an AUC of 245 μM·h and terminal half-life of 2.4 h. The ability to achieve high in vivo plasma concentrations of **29** allowed for the progression of the compound into in vivo efficacy studies.

The effect of compound **29** on blood glucose levels was evaluated in a 21-day study in 6-week-old db/db mice with an oral glucose tolerance test (oGTT) on day 1 and readout on day 21 of glycated hemoglobin (HbA_{1C}). The compound was orally dosed once daily (0.3, 3, 30 mg/kg) to the mice 1 h before the glucose challenge. A dose response was observed for glucose lowering, and statistically significant reductions were apparent at 3 and 30 mg/kg (see Figure 2). The total glucose

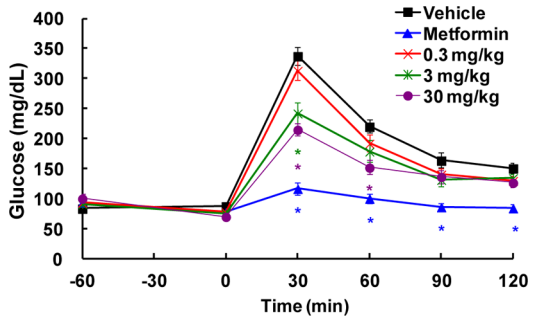

Figure 2. oGTT of compound **29** and metformin in male db/db mice at 6 weeks of age. Metformin was dosed at 300 mg/kg. Glucose AUC reductions were −83% for metformin, −16% for **29** at 0.3 mg/kg, −32% for **29** at 3 mg/kg, and −38% for **29** at 30 mg/kg. ∗ indicates a p value of <0.05.

AUC reductions were 32% and 38%, respectively, which are half the response obtained with high dose metformin treatment (−83%). The magnitude of the response compares well with the maximum reduction in glucose AUC (∼40%) we have achieved over multiple studies with multiple GPR119 agonists and is equivalent to reductions seen with clinical DPPIV inhibitors in this model. After 21 days of treatment, the 30 mg/kg dose of **29** produced a statistically significant reduction in the HbA_{1C} levels comparable to metformin (see Figure 3). In the vehicle-treated animals, HbA_{1C} increased 2.8% while only

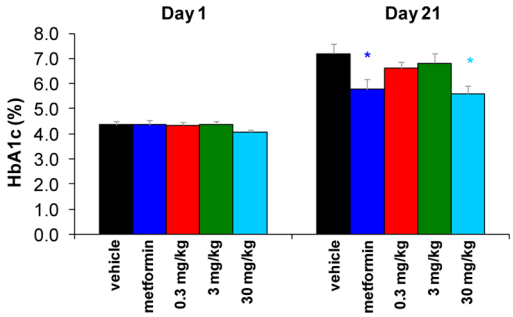

Figure 3. Effects on HbA_{1C} of compound **29** and metformin after 21 days of dosing in male db/db mice starting at 6 weeks of age. Metformin was dosed at 300 mg/kg. The HbA_{1C} reductions related to vehicle were 1.4% for metformin, 0.6% for **29** at 0.3 mg/kg, 0.4% for **29** at 3 mg/kg, and 1.4% for **29** at 30 mg/kg. ∗ indicates a p value of <0.05.

increasing 1.4% in the animals treated with metformin and the 30 mg/kg dose of **29**. Although we were excited to see HbA_{1C} lowering of **29** at 30 mg/kg in a chronic study that was equivalent to metformin, we were concerned about the loss of potency seen in the chronic readout (day 21 HbA_{1C}) as compared to the acute portion (day 1 oGTT) of the study. These results were attributed to the short in vivo half-life of **29** in mice. Low doses (<30 mg/kg) could not provide 24 h of coverage of the EC_{50} to maintain efficacy, and therefore, greater metabolic stability was required to achieve a pharmacokinetic profile suitable for once daily dosing.

COMPOUND OPTIMIZATION AND CLINICAL CANDIDATE SELECTION

Optimization for clinical candidate selection began with metabolite identification experiments to locate the site of oxidation in our lead series. On the basis of experiments with **29** and several other analogs, the metabolic soft spot was identified as the propyl side chain on the pyrimidine. During the optimization of the pyrimidine ring substitution, we had identified several groups that provided much better metabolic stability, such as chloro and trifluoromethyl, but these modifications reduced the in vitro potency by approximately 4- to 5-fold. Therefore, our efforts focused on identifying further in vitro potency improvements, which would allow for the replacement of the propyl group with a more metabolically stable group. The one unexplored area of the original lead was the pyridone ring. Substitution of the 3- or 6-position of the pyridone was not tolerated (see Table 4). However, small

Table 4. In Vitro Activity of Pyridone Analogs

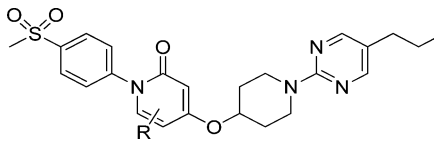

	R	hGPR119 EC_{50}, nM[a]	hGPR119 I.A.[b]
22	H	16	0.8
23	6-Me	>10000	
24	3-Cl	>10000	
25	5-Me	31	0.9
26	5-Ph	>10000	
27	5-CN	12	0.8
28	5-Cl	5	0.8

[a]EC_{50} values were calculated from concentration−response curves. See ref 18 for assay conditions. [b]Reference compound set at 1.0 for each assay run.

substitutions were tolerated at the 5-position, such as methyl (**33**) or cyano (**35**), but large groups, such as phenyl (**34**), ameliorated all activity. The desired potency improvement was achieved with the incorporation of a chloro group (**36**) which provided a ∼3-fold increase in potency versus **29**.

The combination of the metabolically stable 4-trifluoromethylpyrimidine and the 4-chloropyrimidine group with the 5-chloropyridone core produced compounds with the desired potencies (see Table 5). The 4-trifluoromethylpyrimidine (**37**) and the 4-chloropyrimidine (**40**) combined excellent potency with improved human liver microsome half-lives, with a greater than 4-fold improvement for **37** and almost 2-fold for **40** over the original in vivo compound **29**. Concerned that the long metabolic half-life for **37** would cause extended in vivo

dx.doi.org/10.1021/jm501175v | J. Med. Chem. 2014, 57, 7499−7508

Table 5. In Vitro Activity in Final Optimization[a]

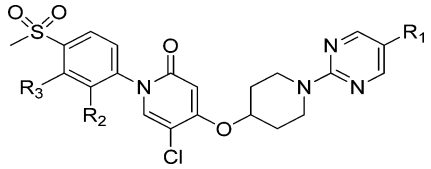

	R_1	R_2	R_3	hEC_{50} (nM)	sol., pH 6.5 (μg/mL)	sol., 50% PEG (μg/mL)	HLM $T_{1/2}$ (min)	mPK $T_{1/2}$ (h)	rPK $T_{1/2}$ (h)
37	CF_3	H	H	13	<1	3	>120	16	>72
38	CF_3	F	H	12	1	122	>120	30	>72
39	CF_3	H	F	16	<1	31	>120	27	>48
40	Cl	H	H	18	<1	7	59	11	9
41	Cl	H	F	13	3	199	39	18	12
42	Cl	F	H	14	<1	41	84	15	22

[a]EC_{50} values were calculated from concentration−response curves. See ref 18 for assay conditions. All intrinsic activities for the GPR119 assay were between 0.8 and 0.9.

exposure, we investigated the entire set of trifuoromethyl substituted compounds in rat pharmacokinetic studies and discovered that they had extremely long half-lives in vivo (greater than 2 days). As we feared, this would translate to an excessively long half-life in humans; the chloropyrimidine derivates (**40**−**42**) were believed to demonstrate a more ideal metabolic profile, exhibiting a good in vitro metabolic stability across species without extended in vivo half-lives in rodents. As such, we focused our selection of a clinical candidate from the chloropyrimidines.

Although **40** appeared to have an ideal liver microsomal stability and in vivo half-life profile, its poor aqueous solubility posed concerns regarding bioavailability (especially at high doses) when administered as a crystalline suspension. Fortunately, we found that use of amorphous spray dried dispersion (SDD) technology[19] could overcome the dissolution issues to provide excellent bioavailability in most cases. In an attempt to rationally apply this technology to our best analogs, we wanted an easy method to determine which compounds had a high likelihood of having excellent bioavailability with SDD formulation. Therefore, in conjunction with the SDD work, we identified a solubility test for this purpose. It was empirically determined that compounds from this chemotype with a solubility of greater than 20 μg/mL in a 50% PEG400/50% PBS solution typically exhibited bioavailabilities of greater than 75%. Interestingly, when the fluorine substituted compounds (**38**, **39**, **41**, **42**) were tested in this solubility screen, all demonstrated much higher solubilities than the des-fluoro analogs **37** and **40**, contrary to normal medicinal chemistry dogma. Although **41** and **42** had the necessary solubility characteristics for SSD formulation, based on its longer human liver microsomal half-life, **42** was chosen for further evaluation as a possible clinical candidate.

Compound **42** had an excellent profile in our vitro safety assays. The molecule demonstrated no significant inhibition (IC_{50} > 40 μM) at nine different cytochrome P450 enzymes, did not activate PXR (EC_{50} > 50 μM), and exhibited no toxicity in a hepatic (HEPG2) cell line at a concentration of 40 μM. Compound **42** was also tested against a panel of 95 GPCRs and enzymes in a broad receptor screening panel and was found to exhibit negligible activity at a concentration of 10 μM. Genotoxicity testing in both the Ames and in vitro micronucleus assay was negative. While the compound inhibits hERG in a patch clamp assay with an IC_{50} of 1.4 μM, it is 99.5% protein bound in human plasma. The reduced plasma free fraction affords a large safety window which was confirmed in both rabbit and cynomolgus monkey electrophysiology studies (data not shown) in which no in vivo effects were seen at a plasma concentration of 20 μM. The rat pharmacokinetic profile of **42** was tested at 1 mg/kg intravenously as a solution and 5 mg/kg orally as a hydroxypropyl methylcellulose (HPMC) SDD loaded at 30% and as a crystalline suspension (see Table 6). When dosed as the SDD formulation, the compound achieved a maximum plasma concentration of 2.7 μM at T_{max} (4 h) with a terminal half-life of 16 h. As predicted by the solubility assay, the bioavailability was high at 87%, whereas the observed bioavailability was low at 33% when dosed as the crystalline suspension. The superior half-life of **42** allowed us to determine if once daily low doses of a potent GPR119 compound can achieve the desired in vivo efficacy responses.

Table 6. Single Dose Plasma Pharmacokinetic Parameters of 42 in Male Sprague-Dawley Rats

dose, iv/po (mg/kg)	1/5
po T_{max} (h)	4
po C_{max} (μM)	2.7
po $T_{1/2}$ (h)	22
po AUC_{tot} (μM·h)	95
po F (%)	33% as suspension
	87% as HMPC SDD
iv Cl (mL min^{-1} kg^{-1})	1.5
iv V_{ss} (L/kg)	2.2

To understand the acute in vivo efficacy of **42**, an oral glucose tolerance test in C57/Bl6 mice was run in a dose response mode (see Figure 4). Statistically significant reductions in glucose were seen at the 30 and 60 min time points for 0.1−1 mg/kg doses and at the 60 min time point for the 0.03 mg/kg dose. The corresponding reductions in glucose AUC were about 40% for all doses at or above 0.1 mg and were statistically significant as compared to vehicle control. Although the data are not presented here, these reductions are similar to those seen with DPPIV inhibitors in this model.

We then examined the ability of **42** to release GLP-1 upon oral glucose administration using a cannulated Sprague−Dawley rat model (see Figure 5). The rats were treated with drug 1 h before an oral glucose bolus, and plasma samples were taken over the subsequent hour. Compound **42** significantly

dx.doi.org/10.1021/jm501175v | J. Med. Chem. 2014, 57, 7499−7508

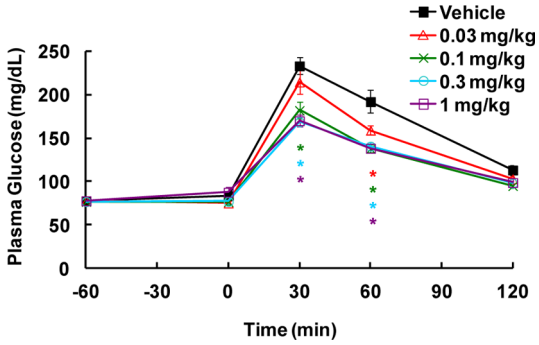

Figure 4. Oral glucose tolerance test of compound **42** in male C57/b6 mice. The glucose AUC reductions versus vehicle control were −14% at 0.03 mg/kg, −37% at 0.1 mg/kg, −39% at 0.3 mg/kg, and −40% at 1 mg/kg. ∗ indicates a p value of <0.05.

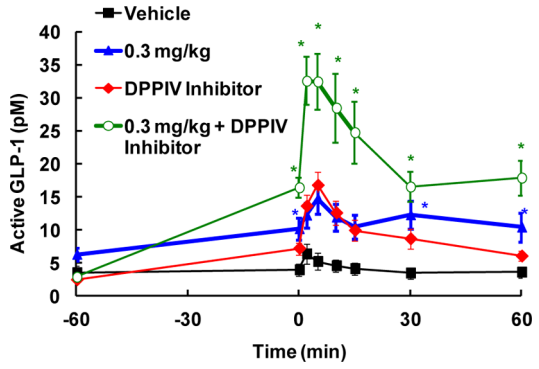

Figure 5. Effect of compound **42**, DPPIV inhibitor,[21] and their combination on active GLP-1 levels in cannulated male Sprague–Dawley rats. ∗ indicates a p value of <0.05.

increased active GLP-1 levels over vehicle at all time points including before glucose bolus. This is consistent with literature reports[10,20] and is equivalent to the response with the DPPIV inhibitor used in this assay. The combination of **42** with the DPPIV inhibitor provided synergistic increases in active GLP-1 at almost all time points including prior to administration of the glucose bolus. These results suggest diabetic patients treated with a GPR119/DPPIV combination might experience dramatic increases in glucose control, perhaps mirroring those seen with GLP-1 injections, but with the convenience of an oral dosing regimen.

The chronic efficacy of **42** was evaluated in the 3-week db/db mouse model used previously in the evaluation of **29**. However, the efficacy end points were changed to fasting plasma glucose and fasting plasma insulin. The once daily doses were chosen to bracket the activity seen in the acute mouse oGTT study. Statistically significant reductions in fasting plasma glucose on day 21 were seen at doses as low as 0.03 mg/kg (see Figure 6). Unfortunately, because of a handling error that required the removal of 6 of 10 animals, the 0.1 mg/kg dose did not achieve significance. In the measurement of the fasting plasma insulin on day 21 (Figure 7), elevations in insulin concentration were seen at all doses of **42**, whereas the insulin levels of the vehicle animals had dropped 2-fold, even though the glucose levels had risen dramatically. The preservation of the animal's ability to secrete insulin suggests that compound **42** might be preventing the β-cell mass depletion normally seen in this rapidly progressing diabetes model. It should be noted that the effects on glucose parameters were seen without any weight loss in any

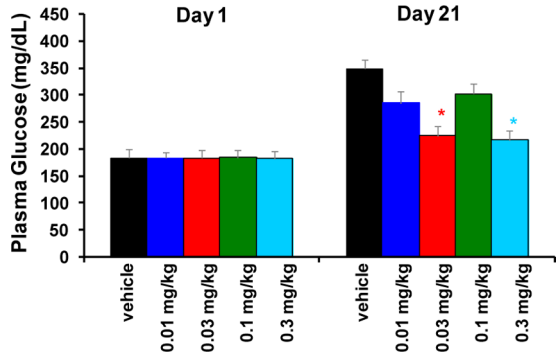

Figure 6. Effect on fasting plasma glucose levels of compound **42** after 21 days of dosing in male db/db mice starting at 6 weeks of age. The plasma glucose reductions relative to vehicle were 18% at 0.01 mg/kg, 36% at 0.03 mg/kg, 13% at 3 mg/kg, and 38% at 30 mg/kg. ∗ indicates a p value of <0.05.

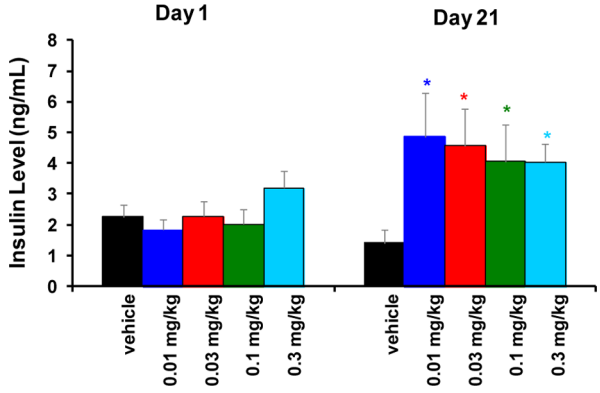

Figure 7. Effect on fasting plasma insulin levels of compound **42** after 21 days of dosing in male db/db mice starting at 6 weeks of age. ∗ indicates a p value of <0.01.

of the drug treated groups. The combination of acute efficacy in the GLP-1 elevation studies and the potent activity demonstrated in the chronic efficacy model led us to choose compound **42** for progression into development and ultimately phase 1 clinical trials.

■ CHEMISTRY

The synthesis of compound **42** and analogs described above was achieved in a straightforward four-step route (Scheme 1). In the case of **42**, the synthesis began with the coupling of gimeracil with the protected 4-hydroxypiperidine under standard Mitsunobu conditions to yield intermediate **43**. 1,2-Difluoro-4-methylsulfonylbenzene was reacted with the sodium salt of **43** in dimethylformamide. After the mixture was heated to 130 °C for 2 h, intermediate **44** was isolated. The protecting group of **44** was removed with aqueous hydrogen chloride to yield the piperidine hydrochloride salt, **45**. The synthesis was completed by coupling **45** to 5-chloro-2-iodopyrimidine in dimethylformamide with diisopropylethylamine to yield **42**. The compounds from this series could also be prepared by a simple rearrangement of the reaction order, such as precoupling the pyrimidine with the piperidine before the Mitsunobu reaction with gimeracil followed by coupling with the methylsulfonylphenyl group.

dx.doi.org/10.1021/jm501175v | J. Med. Chem. 2014, 57, 7499–7508

Scheme 1. Synthesis of 42

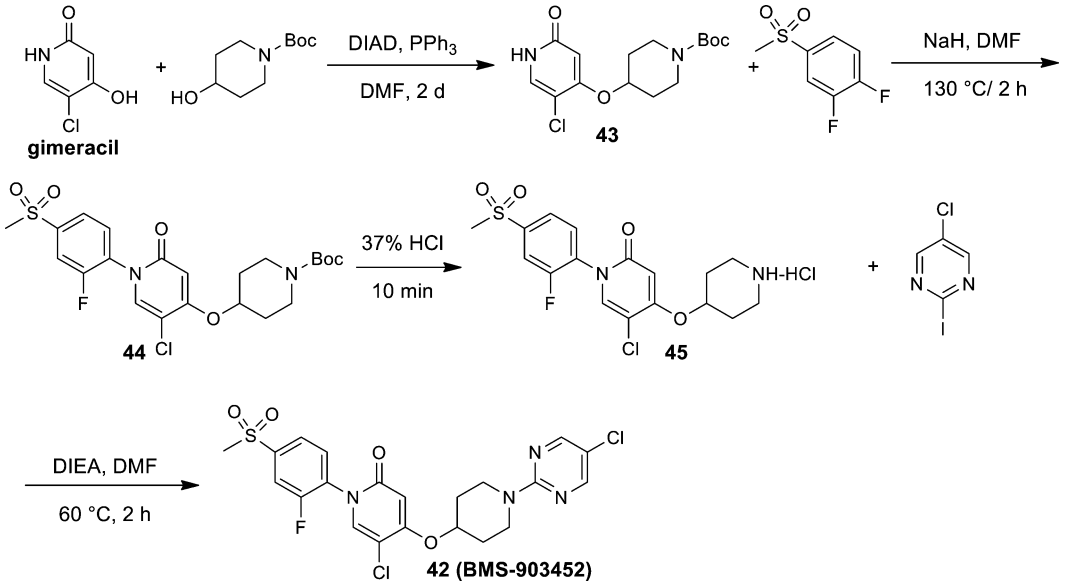

CLINICAL TRIAL RESULTS

A phase 1 clinical trial with **42** has been conducted as a single ascending dose study in normal healthy volunteers under a double-blind, placebo controlled protocol to determine plasma exposure and tolerability. The doses were escalated from 0.1 to 120 mg of drug with the first two doses given as solutions and the remainder given as SDD suspensions. Compound **42** was safe and well tolerated at all doses, with plasma exposure (see Figure 8) increasing in a dose proportional manner. The terminal half-life was determined to be between 36 and 51 h. The pharmacokinetic profile shows increases in drug plasma concentrations at 10 and 24 h in every dose panel. These time points correspond to meal time for the patients and indicate possible enterohepatic recirculation of the drug. This provides one the chance to speculate that the addition of drug to the gastrointestinal tract every time a patient consumes glucose could provide efficacy benefits from the activation of the GPR119 receptors in the GI tract.

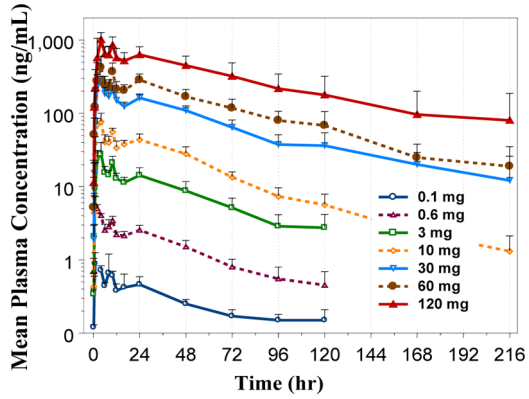

Figure 8. Pharmacokinetics of compound **42** orally dosed in normal healthy human volunteers. The 0.1 and 0.6 mg doses were given as oral solutions, and doses of 3 mg and above were given as oral suspension of an amorphous spray−dried dispersion.

In the phase 1 study, efficacy readouts such as glucose levels and GLP-1 levels were measured over 24 h, even though there was little expectation to see changes in normal healthy volunteers who have robust glucose control mechanisms. As expected, there was no change in the 24 h AUC for glucose from the day before drug treatment to the first day following drug treatment (data not shown). However, there was a nonstatistically significant trend for increases in total GLP-1 AUC levels over the first 24 h (see Figure 9). With a dose as low as 0.6 mg, there is a 20% increase in total GLP-1 AUC and a dose dependent response up to a plateau of ∼50% AUC increase with the 10 mg and higher dose panels. Although the data are not a robust response and have no statistical value, even a trend in the correct direction in healthy volunteers is encouraging and data from diabetic patients are eagerly awaited.

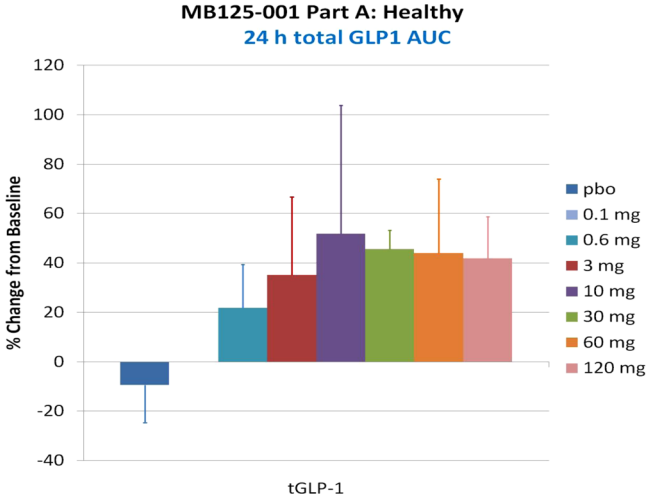

Figure 9. Effects of compound **42** on total GLP-1 area under the curve over 24 h. Data are expressed as percent change in total GLP-1 AUC between day −1 and day 1 in six patients at each dose.

EXPERIMENTAL SECTION

General Methods. For anhydrous reactions DRISOLV solvents from EMD were used. For other reactions reagent or HPLC grade solvents were used. All commercially available solvents and reagents

dx.doi.org/10.1021/jm501175v | J. Med. Chem. 2014, 57, 7499−7508

were used as received. All reactions were carried out under an argon atmosphere unless noted otherwise. Reaction mixtures were concentrated under reduced pressure at 40−65 °C on a rotary evaporator. Analytical thin layer chromatography (TLC) was performed on silica gel 60 F_{254} plates from Merck. Flash column chromatography separations were preformed on RediSep normal phase silica flash columns (230−400 mesh, 60 Å, Teledyne ISCO). LC−MS measurements were obtained using either a Shimadzu HPLC system with a Phenomenex Luna C18 column (5 μm, 100 Å, 4.6 mm × 30 mm), operated at 40 °C with 0.1% TFA modified ACN/water mobile phases or a Waters Acquity UPLC system with an Acquity UPLC BEH C18 (1.7 μm, 130 Å, 2.1 mm × 50 mm) column operated at 50 °C with 0.05% TFA modified ACN/water mobile phases. UV detection was carried out with a Shimadzu SPD-10AV at 220 nm, and mass detection was carried out with Waters ZQ single quadrupole mass spectrometer hybrid system using positive electrospray ionization.

Final HPLC purity determination was made with a Shimadzu HPLC system, with a Waters Sunfire C18 (3.5 μm, 100 Å, 3.0 mm × 150 mm) column and a Waters Xbridge phenyl (3.5 μm, 130 Å, 3.0 mm × 150 mm) column with 0.05% TFA modified ACN/water mobile phases with gradient run from 10% to 90% ACN. UV detection was carried out with a Shimadzu SPD-20AV at 220 and 254 nm. All final compounds achieved a minimum of 95% purity. All chromatography was carried out with HPLC grade organic solvents. ^{1}H NMR spectra were obtained on a Bruker 400 MHz spectrometer using the indicated solvent. Chemical (δ) shifts are reported in ppm from tetramethylsilane with the residual solvent signal as the internal standard; signals are expressed as s = singlet, d = doublet, t = triplet, q = quartet, m = multiplet, and br = broad. Coupling constants (J) are in hertz (Hz).

All animals were treated according to the standards of the BMS Animal Care and Use Committee (ACUC). Animals were maintained at the Bristol-Myers Squibb animal facilities (Hopewell, NJ) with 12 h light/dark cycle and free access to food and water. The animals were fed ad libitum normal chow.

***tert*-Butyl 4-((5-Chloro-2-oxo-1,2-dihydropyridin-4-yl)oxy)-piperidine-1-carboxylate (43).** To an ice-cooled mixture of 5-chloro-4-hydroxypyridin-2(1*H*)-one (11.86 g, 81 mmol), *tert*-butyl 4-hydroxypiperidine-1-carboxylate (16.40 g, 81 mmol), and triphenylphosphine (23.51 g, 90 mmol) in a mixture of DMF (55 mL) and THF (55 mL) was added dropwise a solution of (*E*)-diisopropyl diazene-1,2-dicarboxylate (17.65 mL, 90 mmol) in THF (50 mL) over 30 min. The mixture was allowed to warm to room temperature and stirred for 2 days. The reaction mixture was concentrated in vacuo to give a yellow oil. The oil was dissolved in EtOAc (300 mL), washed with saturated $NaHCO_3$ (150 mL), and the organic layer was concentrated in vacuo. The residue was purified by flash column chromatography. The column was initially eluted with EtOAc in DCM (0−100%) until the impurities were off the column, and the mobile phase was switched to MeOH in DCM (0−10%) to collect **43** (14.7 g, 55%) as a white solid. ^{1}H NMR (400 MHz, $CDCl_3$) δ ppm 12.98 (br s, 1 H), 7.35 (s, 1 H), 5.92 (s, 1 H), 4.51−4.63 (m, 1 H), 3.57−3.68 (m, 2 H), 3.43−3.54 (m, 2 H), 1.79−2.00 (m, 4 H), 1.48 (s, 9 H). LC−MS: m/z = 329.0 [M + H].

***tert*-Butyl 4-(5-Chloro-1-(2-fluoro-4-(methylsulfonyl)-phenyl)-2-oxo-1,2-dihydropyridin-4-yloxy)piperidine-1-carboxylate (44).** To a solution of *tert*-butyl 4-(5-chloro-2-oxo-1,2-dihydropyridin-4-yloxy)piperidine-1-carboxylate (**43**) (1.93 g, 5.87 mmol) in DMF (15 mL) was added portionwise sodium hydride (60% w/w in mineral oil, 0.282 g, 7.04 mmol) over a period of 5 min. The mixture was stirred at room temperature for 30 min, followed by the addition of 1,2-difluoro-4-(methylsulfonyl)benzene (1.47 g, 7.63 mmol). The reaction mixture was heated at 130 °C for 2 h, cooled to room temperature, and quenched by the addition of H_2O (200 mL). The quenched reaction mixture was extracted with EtOAc (200 mL). The organic layer was concentrated in vacuo. The residue was purified by flash column chromatography (0−100% EtOAc in DCM), with the unwanted O-isomer eluting before the desired N-isomer, to give **44** (1.31 g, 45%) as a white solid. ^{1}H NMR (400 MHz, $CDCl_3$) δ ppm 7.82−7.91 (m, 2 H), 7.62 (dd, J = 6.78, 8.53 Hz, 1 H), 7.32 (s, 1 H), 6.03 (s, 1 H), 4.57−4.64 (m, 1 H), 3.59−3.68 (m, 2 H), 3.46−3.55 (m, 2 H), 3.11 (s, 3 H), 1.84−2.02 (m, 4 H), 1.48 (s, 9 H). LC−MS: m/z = 501.2 [M + H].

5-Chloro-1-(2-fluoro-4-(methylsulfonyl)phenyl)-4-(piperidin-4-yloxy)pyridin-2(1*H*)-one, HCl (45). A mixture of *tert*-butyl 4-(5-chloro-1-(2-fluoro-4-(methylsulfonyl)phenyl)-2-oxo-1,2-dihydropyridin-4-yloxy)piperidine-1-carboxylate (**44**) (1.31 g, 2.62 mmol) and HCl (37% aq, 5.00 mL, 60.9 mmol) was stirred at room temperature for 15 min. The reaction mixture was concentrated in vacuo to give **45** (1.15 g, 2.62 mmol, 100% yield) as a white solid. ^{1}H NMR (400 MHz, DMSO-d_6) δ 8.96 (br s, 2H), 8.12 (s, 1H), 8.02 (dd, J = 1.76, 9.24 Hz, 1H), 7.88−7.94 (m, 1H), 7.79−7.87 (m, 1H), 6.31 (s, 1H), 4.80−4.92 (m, 1H), 3.35 (s, 3H), 3.16−3.26 (m, 2H), 3.03−3.16 (m, 2H), 2.10−2.23 (m, 2H), 1.86−1.99 (m, 2H). LC−MS: m/z = 401.1 [M + H].

5-Chloro-4-(1-(5-chloropyrimidin-2-yl)piperidin-4-yloxy)-1-(2-fluoro-4-(methylsulfonyl)phenyl)pyridin-2(1*H*)-one (42). To a solution of 5-chloro-1-(2-fluoro-4-(methylsulfonyl)phenyl)-4-(piperidin-4-yloxy)pyridin-2(1*H*)-one, HCl (**45**) (1.15 g, 2.62 mmol) and DIEA (1.37 mL, 7.85 mmol) in DMF (10 mL) was added 5-chloro-2-iodopyrimidine (0.755 g, 3.14 mmol). The reaction mixture was heated at 60 °C for 4 h. The reaction mixture was concentrated in vacuo to give a yellow oil. The oil was dissolved in EtOAc (200 mL) and washed with saturated $NaHCO_3$ (200 mL), and the organic layer was concentrated in vacuo. The residue was purified by flash column chromatography (0−100%, EtOAc in DCM) to give the title compound as an off-white solid. To increase the purity of the isolated solid, the solid was added to MeOH (250 mL) and refluxed for 6 h. The slurry was cooled to 4 °C, filtered, washed with MeOH (100 mL), and dried in vacuo giving **42** (0.934 g, 1.82 mmol, 69.5% yield) as a white solid. ^{1}H NMR (400 MHz, $CDCl_3$) δ 8.25 (s, 2H), 7.82−7.94 (m, 2H), 7.63 (dd, J = 6.65, 8.41 Hz, 1H), 7.33 (d, J = 1.00 Hz, 1H), 6.07 (s, 1H), 4.70 (tt, J = 3.39, 6.53 Hz, 1H), 3.98−4.08 (m, 2H), 3.87−3.96 (m, 2H), 3.12 (s, 3H), 2.02−2.11 (m, 2H), 1.92−2.01 (m, 2H). LC−MS: m/z = 513.0 [M + H].

21-Day db/db Mouse Study. A cohort of 90 male BKS Cg-m+/+ Lepr db/db/J mice (5 weeks of age at arrival) purchased from Jackson Laboratories (Bar Harbor, ME) was acclimated to the vivarium for 1 week prior to study start. Two days before the study date, mice were randomized to day 1 or day 2 oGTT based on fed blood glucose and HbA1c levels, measured by glucometer (Accu-Check) and COBAS Mira, respectively, via tail nick. Following an overnight fast, mice were randomized to treatment based on their blood glucose and body weights. After 40 min in adaptation to the new group, mice were bled again for blood glucose level at the −60 min time point, and 5 μL of whole blood was collected into a COBAS tube containing 250 μL of hemolysate reagent for determination of HbA1c. After the blood collection, mice received vehicle (40% PEG 400, 10% Cremophor, and 50% water) or compound **29** orally (5 mL/kg). At 60 min after dosing, an additional glucose measurement was taken. Immediately after the 0 min time point collection, mice were given an oral glucose challenge with 50% dextrose (4 mL/kg). Plasma glucose was measured at 30, 60, 90, and 120 min after the glucose challenge. Mice were then returned to home cages and given free access to food and water. From day 2 to day 21, mice were orally dosed with the vehicle or compound once daily at 9:00 a.m. After day 21 of dosing, mice were fasted overnight and fasting plasma glucose and HbA1c were measured at 24 h after dose, followed by a day 22 dosing in which trunk blood from three mice of each group was collected for PK analysis by decapitation under anesthesia with CO_2 3.5 h after compound administration. All blood samples (except the 5 μL blood for HbA1c) were centrifuged at 8000 rpm at 4 °C for 10 min. Remaining mice (seven mice in each group) were returned to home cage and given access to food and water. The 24 h postdose plasma levels of compounds from trunk blood were determined as well.

Mouse Acute Oral Glucose Tolerance Test Assay. Male C57BL/6J mice (8 weeks of age at arrival) from Jackson Laboratories (Bar Harbor, ME) were single-housed and had free access to normal chow (Teklad 2018) and water ad libitum. They were allowed to acclimate to the animal facilities for 2 weeks. The mice were fasted

dx.doi.org/10.1021/jm501175v | J. Med. Chem. 2014, 57, 7499−7508

overnight before the study. On the morning of the experiment day, the mice (10 weeks of age) were acclimated to the lab for 3 h before the baseline plasma glucose values and body weights were collected. Whole blood was obtained via tail nick, and the fasting plasma glucose was determined via glucometer (Accu-check, Aviva, Roche). Mice were randomized based on fasting plasma glucose and body weight and assigned to either vehicle or one of the treatment groups (n = 8/group). The plasma glucose baseline values were obtained at the −60 min time point immediately prior to dosing with vehicle (40% PEG 400, 10% Cremophor, and 50% water) or **42** (10 mL/kg) in vehicle. Plasma glucose values were determined again at 60 min after initial dose (0 time point), before a bolus of oral glucose (2 g/kg, 8 mL/kg) was given to the mice. Plasma glucose samples were collected again at 30, 60, and 120 min after glucose challenge, respectively. At 3.5 h postdrug dose, mice were decapitated and the trunk blood was collected. The blood samples were centrifuged at 8000 rpm for 10 min at 4 °C. An aliquot of 200 μL plasma sample was separated from each blood sample and stored at −80 °C.

Cannulated Rat GLP-1 Assay. Male Sprague−Dawley (SD) rats (body weight, 250−275g) with carotid artery cannulation (CAC) were obtained from Charles River Laboratories (Wilmington, MA). Additional age-matched noncannulated SD rats (donor rats) were used to obtain blood in order to replace blood taken from CAC rats during the study. Overnight fasted donor rats were anesthetized by isofluorane. From each donor rat, 8−10 mL of blood was collected by cardiac puncture. The donor blood was transferred to a vial containing heparin solution with a final concentration of 20 U/mL. For the glucose tolerance test, overnight fasted CAC rats (n = 10/group) were connected to extension PE50 tubing. The lock solution was withdrawn, and the line was flushed with heparinized saline (20 U/mL). The animals were allowed to acclimate for 60 min before the baseline blood sample was taken. Blood samples (0.5 mL each) were collected at each time point (−60, 0, 2, 5, 10, 15, 30, and 60 min) through the carotid artery line into 1 mL hematology tubes coated with EDTA and a complex of aprotinin and protease cocktail enzyme inhibitors (Sigma, St. Louis, MO) at a final concentration of 40 U/mL. Plasma glucose levels were measured at these time points during the study via glucometer (Accu-check, Aviva, Roche Diagnostics, Indianapolis, IN). Rats were randomized into either vehicle or one of the treatment groups based on fasting plasma glucose values at the −60 min time point. Following randomization, rats were dosed with vehicle (40% PEG 400, 10% Cremophor, and 50% water) or **42**. One hour later, a bolus of glucose (2 g/kg, 4 mL/kg) was given at 0 min time point after a blood sample was taken. Blood samples were kept on ice until processed. Blood samples were centrifuged at 8000 rpm for 10 min at 4 °C. The plasma samples were harvested and kept at −80 °C until used for GLP-1 assessment.

Second 21-Day db/db Mouse Study. A cohort of male BKS Cg-m+/+ Lepr db/db/J mice (5 weeks of age at arrival) was purchased from Jackson Laboratories (Bar Harbor, ME). They were allowed to acclimate to the animal facility for 2 weeks. They were housed 5 per cage and had free access to normal chow (Teklad 2018) and water ad libitum The mice (7 weeks of age) were fasted overnight. The next morning, their fasting body weight was recorded and blood samples were collected in EDTA tubes via tail nick for determination of plasma glucose and insulin levels. The blood samples were centrifuged at 8000 rpm for 10 min at 4 °C. The fasting plasma glucose levels were determined by a COBAS clinical chemistry analyzer (Roche Diagnostics, Indianapolis, IN). The samples were frozen, and plasma insulin was determined by ELISA at a later time. The 60 mice were randomized into the vehicle group or one of the treatment groups (n = 8/group). Following 3 weeks of dosing with vehicle (40% PEG 400, 10% Cremophor, and 50% water) or compound **42** orally (5 mL/kg) (after the 21st dose was given), animals were fasted. On day 22, the fasting body weight, plasma glucose, and insulin levels were determined 24 h after the 21st dose. In order to assess plasma exposure of the compound, the mice were dosed again after the blood samples were collected for glucose and insulin. Blood was collected at 3 and 24 h after dose, and plasma concentrations of **42** were determined in these samples.

Blood Sample Collection and Analysis. *Glucose Assay.* A COBAS clinical analyzer (Roche) was used to measure glucose levels in the plasma in the db/db mouse study with **42**. An Accu-check glucometer (Roche) was used to determine plasma glucose from blood samples collected from tail bleed in the C57BL/6J and SD rat studies to get the immediate reading.

GLP-1 Assay. An aliquot (200 μL) of plasma was transferred into a prechilled Eppendorf tube. Tubes were kept on dry ice and then stored at −80 °C until used in assays for GLP-1 and insulin. Plasma active GLP-1 was measured using a glucagon-like peptide-1 (active) ELISA kit (LINCO Research, St. Charles, MO). The samples were tested according to the manufacturer's instruction for 100 μL per sample protocol.

Insulin Assay. An aliquot (200 μL) of plasma was transferred into a prechilled Eppendorf tube. Tubes were kept on dry ice and then stored at −80 °C until used in assays for GLP-1 and insulin. Plasma insulin was measured by Mercodia rat or mouse ultrasensitive insulin ELISA (Mercodia, Winston-Salem, NC). The samples were tested according to the manufacturer's instructions for 5 μL per sample.

HbA1c Assay. Blood HbA1c levels were determined by a COBAS clinical analyzer (Roche Diagnostics, Indianapolis, IN).

■ ASSOCIATED CONTENT

Ⓢ Supporting Information

Synthetic procedures for analogs of **42**. This material is available free of charge via the Internet at http://pubs.acs.org.

■ AUTHOR INFORMATION

Corresponding Author

*Phone: 609-818-5381. E-mail: dean.wacker@bms.com.

Author Contributions

The manuscript was written through contributions of all authors. All authors have given approval to the final version of the manuscript.

Notes

The authors declare no competing financial interest.

■ ABBREVIATIONS USED

GPR119, G-protein-coupled receptor 119; GLP-1, glucagon-like peptide 1; GIP, glucose-dependent insulinotropic polypeptide; GPCR, G-protein-coupled receptor; PXR, pregnane X receptor; HEPG2, human liver carcinoma cell line; hERG, human ether-a-go-go-related gene; PAMPA, parallel artificial membrane permeability assay; AUC, area under curve; oGTT, oral glucose tolerance test; HbA_{1C}, hemoglobin A_{1C}; DPPIV, dipeptidyl peptidase 4; PEG, polyethylene glycol; SDD, spray dried dispersion; PBS, phosphate buffered saline; HPMC, hydroxypropyl methylcellulose

■ REFERENCES

(1) International Diabetes Federation, Diabetes Atlas. http://www.idf.org/sites/default/files/EN_6E_Atlas_Full_0.pdf, 2013

(2) Centers for Disease Control and Prevention, National Diabetes Fact Sheet, 2011. http://www.cdc.gov/diabetes/pubs/pdf/ndfs_2011.pdf, 2011

(3) Koro, C. E.; Bowlin, S. J.; Bourgeois, N.; Fedder, D. O. Glycemic control from 1988 to 2000 among U.S. adults diagnosed with type 2 diabetes. *Diabetes Care* **2004**, *27*, 17−20.

(4) Philippe, J.; Raccah, D. Treating type 2 diabetes: How safe are current therapeutic agents? *Int. J. Clin. Pract.* **2009**, *63*, 321−332.

(5) Holst, J. J.; Vilsboll, T.; Deacon, C. F. The incretin system and its role in type 2 diabetes mellitus. *Mol. Cell. Endocrinol.* **2009**, *297*, 127−136.

(6) Brubaker, P. L. Update on incretin biology: focus on glucagon-like peptide 1. *Endocrinology* **2010**, *151*, 1984−1989.

(7) Fredriksson, R.; Hoglund, P. J.; Gloriam, D. E. I.; Lagerstrom, M. C.; Schioth, H. B. Seven evolutionarily conserved human rhodopsin G protein-coupled receptors lacking close relatives. *FEBS Lett.* **2003**, *554*, 381−388.
(8) Soga, T.; Ohishi, T.; Matsui, T.; Saito, T.; Matsumoto, M.; Takasaki, J.; Matsumoto, S.; Kamohara, M.; Hiyama, H.; Yoshida, S.; Momose, K.; Ueda, Y.; Matsushime, H.; Kobori, M.; Furuichi, K. Lysophosphatidylcholine enhances glucose-dependent insulin secretion via an orphan G-protein-coupled receptor. *Biochem. Biophys. Res. Commun.* **2005**, *326*, 744−751.
(9) Chu, Z.-L.; Jones, R. M.; He, H.; Carroll, C.; Gutierrez, V.; Lucman, A.; Moloney, M.; Gao, H.; Mondala, H.; Bagnol, D.; Unett, D.; Liang, Y.; Demarest, K.; Semple, G.; Behan, D. P.; Leonard, J. A role for β-cell-expressed G protein-coupled receptor 119 in glycemic control by enhancing glucose-dependent insulin release. *Endocrinology* **2007**, *148*, 2601−2609.
(10) Chu, Z.-L.; Carroll, C.; Alfonso, J.; Gutierrez, V.; He, H.; Lucman, A.; Pedraza, M.; Mondala, H.; Gao, H.; Bagnol, D.; Chen, R.; Jones, R. M.; Behan, D. P.; Leonard, J. A role for intestinal endocrine cell-expressed G protein-coupled receptor 119 in glycemic control by enhancing glucagon-like peptide-1 and glucose-dependent insulinotropic release. *Endocrinology* **2008**, *149*, 2038−2047.
(11) Overton, H. A.; Babbs, A. J.; Doel, S. M.; Fyfe, M. C. T.; Gardner, L. S.; Griffin, G.; Jackson, H. C.; Procter, M. J.; Rasamison, C. M.; Tang-Christensen, M.; Widdowson, P. S.; Williams, G. M.; Reynet, C. Deorphanization of a G protein-coupled receptor for oleoylethanolamide and its use in the discovery of small-molecule hypohagic agents. *Cell Metab.* **2006**, *3*, 167−175.
(12) Jones, R. M.; Semple, G.; Xiong, Y.; Shin, Y.-J.; ren, A. S.; Calderon, I.; Fioravant, B.; Choi, J. S. K.; Sage, C. R. Preparation of fused aryl and heteroaryl derivatives, in particular pyrazolo[3,4-*d*]pyrimidines, as modulators of G-coupled protein receptor and their use in the prophylaxis and treatment of metabolic disorders. World Patent Application WO 2005/007658, January 27, 2008.
(13) Semple, G.; Lehmann, J.; Wong, A.; Ren, A.; Bruce, M.; Shin, Y. J.; Sage, C. R.; Morgan, M.; Chen, W.-C.; Sebring, K.; Chu, Z.-L.; Leonard, J. N.; Al-Shamma, H.; Grottick, A. J.; Du, F.; Lian, Y.; Demarest, K.; Jones, R. M. Discovery of a second generation of the orphan G-protein coupled receptor GPR119 with an improved profile. *Biorg. Med. Chem. Lett.* **2012**, *22*, 1750−1755.
(14) Thomas Reuters Drug News. http://drugnews.thomsonpharma.com/ddn/home.do.
(15) McWherter, C. Presented at the 32nd Annual National Medicinal Chemistry Symposium, Minnesota, MN, June 6−9, 2010; Oral Session 2.
(16) Carpenter, A. J. Presented at the 32nd Annual National Medicinal Chemistry Symposium, Minnesota, MN, June 6−9, 2010; Oral Session 2.
(17) PSN821 structure has not been disclosed. Its close lead PSN408 was disclosed; see the following: The 32nd Annual National Medicinal Chemistry Symposium, Minnesota, MN, June 6−9, 2010; Oral Session 2.
(18) Ye, X.-Y.; Morales, C. L.; Wang, Y.; Rossi, K. A.; Malmstrom, S. E.; Abousleiman, M.; Sereda, L.; Apedo, A.; Robl, J. A.; Miller, K. J.; Krupinski, J.; Wacker, D. A. Synthesis and structure−activity relationship of dihydrobenzofuran derivatives as novel human GPR119 agonists. *Bioorg. Med. Chem. Lett.* **2014**, *24*, 2539−2545.
(19) Friesen, D. T.; Shanker, R.; Crew, M.; Smithey, D. T.; Curatolo, W. J.; Nightingale, J. A. S. Hydroxypropyl methylcellulose acetate succinate-based spray-dried dispersions: an overview. *Mol. Pharmaceutics* **2008**, *5*, 1003−1019.
(20) Lauffer, L. M.; Iakoubov, R.; Brubaker, P. L. GPR119 is essential for oleoylethanolamide-induced glucagon-like peptide-1 secretion from the intestinal enteroendocrine L-cell. *Diabetes* **2009**, *58*, 1058−1066.
(21) Compound **48** from following reference was used as the DPPIV inhibitor in the study: Simpkins, L. M.; Bolton, S.; Pi, Z.; Sutton, J. C.; Kwon, C.; Zhao, G.; Magnin, D. R.; Augeri, D. J.; Gungor, T.; Rotella, D. P.; Sun, Z.; Liu, Y.; Slusarchyk, W. S.; Marcinkeviciene, J.; Robertson, J. G.; Wang, A.; Robl, J. A.; Atwal, K. S.; Zahler, R. L.; Parker, R. A.; Kirby, M. S.; Hamann, L. G. Potent non-nitrile dipeptidic dipeptidyl peptidase IV inhibitors. *Bioorg. Med. Chem. Lett.* **2007**, *17*, 6476−6480.